

Comparative Analysis of Stator Resistance Estimators in DTC-CSI Fed IM Drive

M.Sivakumar¹, T.Thanakodi², N.Panneer Selvam³

^{1,2} Valivam Desikar Polytechnic College, Nagapattinam, Tamilnadu-639111, India.

³M..A.M.Polytechnic College, Trichirappalli, Tamilnadu-621105, India.

Abstract

Stator resistance is the most importance to estimate torque, flux in direct torque controlled sensorless speed controlled induction motor drives. During low speed operation stator resistance inevitably varies due to temperature and low frequency. For stable and accurate operation at low speed requires an appropriate on-line identification algorithm for the stator resistance. This paper proposed to analyze stator resistance estimation by using proportional integral (PI) and MRAS schemes in CSI fed Induction motor drive with direct torque control during low speed operation. The performances of the two control schemes are evaluated in terms of torque, Speed and flux. The analysis has been carried out on the basis of the results obtained by MATLAB/simulink and hardware implementation.

Keywords: Current source Inverter, Direct torque control, Sensorless Speed, Stator resistance estimation, Digital signals processing.

INTRODUCTION

HIGH-POWER medium-voltage drives applications [1], the current-source inverter (CSI) fed drives are used increasingly. The current source inverters having simple converter topology, inherent four-quadrant operation, reliable fuse less short circuit protection, and motor friendly waveforms (with low dv/dt). Further improve the system performance, research efforts on CSI fed drives have been recently put on new current-source drive topology, advanced modulation scheme development [2]–[7], control performance [8]–[11], and efficiency [12], [13], etc.

DTC is recently developed in industrial drives due to generating fast torque responses. In DTC, the stator resistance

is used to estimate the stator flux [14], [15]. The stator resistance is varying due to changes in temperature and low frequency; make the system becomes unstable at low speeds.

An accurate value of the stator resistance is of crucial importance for correct operation of a sensorless drive in the low speed region, since any mismatch between the actual value and estimated value may lead not only to a substantial speed estimation error but to instability as well [16]. As a consequence, numerous on-line schemes for stator resistance estimation have been proposed in recent past [16-27].

In this paper the PI and MRAS based compensation of stator resistance are analyzed for DTC-CSI fed induction motor during low speed operation and its performance results are verified by software and hardware.

SYSTEM CONFIGURATION AND CONTROL

Figure 1 shows the main circuit of the DTC-CSI-fed induction motor drive. L_L and C_L are the inductance and capacitance of the line filter and C_M is the filter capacitance in motor side. L_d is a smoothing inductor which is to minimize the current bearing problems of the motor drive [28]. Both the rectifier and the inverter are controlled with PWM and direct torque controller (DTC) respectively. The line side rectifier, left part in Figure 1 has to control the dc link current via the line side dc link voltage. Disturbance value is the machine side dc link voltage, produced by the induction machine via the inverter, right part in Figure 1. The control performance is basically influenced by the dc link inductance. The machine side inverter has to control the current in the motor to adjust the motor torque to the reference value. This is mainly a phase control, as the current amplitude in the machine is given according to the amplitude of the dc link current controlled by the rectifier.

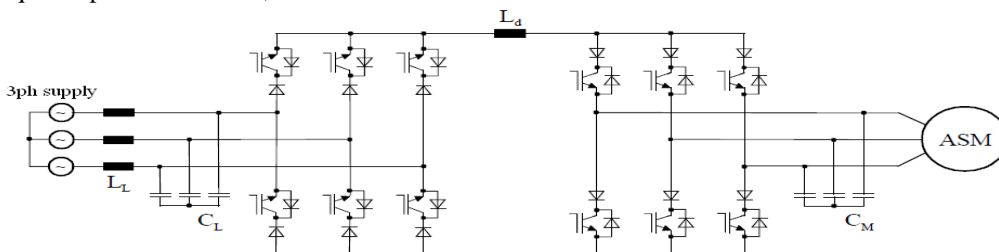


Figure 1. Current source converter induction machine drive

Flux, Torque estimation

The functional block diagram of the Sensorless vector controlled drive is shown in Figure 2. It shown that the vector control algorithm requires rotor flux position θ_f , which can be estimated from the stator flux space vector, λ_s is estimated using

$$\lambda_s = \int (V_s - R_s i_s) dt \quad (1)$$

Where V_s and i_s are the stator voltage and current space vectors. Superscript indicates that the variables are referred to stator axis. The rotor flux vector, λ_r is obtained by subtracting the leakage flux from the stator flux vector as in

$$\lambda_r = \int \frac{L_m}{L_r} [V_s - (R_s + \sigma L_s p) i_s] \quad (2)$$

Where

$$\sigma = 1 - \frac{L_m^2}{L_s L_r}$$

σ – Leakage factor

L_s – Stator self Inductance

L_r – Rotor self Inductance and

L_m - magnetizing inductance,

The rotor flux, rotor position angle, Torque is estimated from the stator voltage and current.

$$\theta_f = \tan^{-1} \left(\frac{\lambda_{ds}}{\lambda_{qs}} \right) \quad (3)$$

$$T_e = \frac{3}{2} p (\lambda_{ds} i_{qs} - \lambda_{qs} i_{ds}) \quad (4)$$

The available stator resistance on-line identification schemes can be classified into a couple of distinct categories. In general, all the methods rely on stator current measurement and predominantly require information regarding stator voltages as well. As illustrated in Figure 2 the outputs of the flux and speed controllers are the synchronous frame d -axis stator current Reference (I_{ds}^*) and the reference torque (T_e^*), respectively, where the torque subsequently generates the q -axis stator current reference (I_{qs}^*). After the motor-side capacitor current compensation, the command inverter currents in the synchronous d - q frame (I_{dw} , I_{qw}) are obtained, which is generate the desired dc-link current (i_{dc}^*) and the inverter switching angle (θ_f). The CSI output current magnitude is regulated by controlling the dc-link current through the CSR, while the CSI operates with DTC switching table. The torque error and an adjustable phase angle θ_{inv} are the input of switching table.

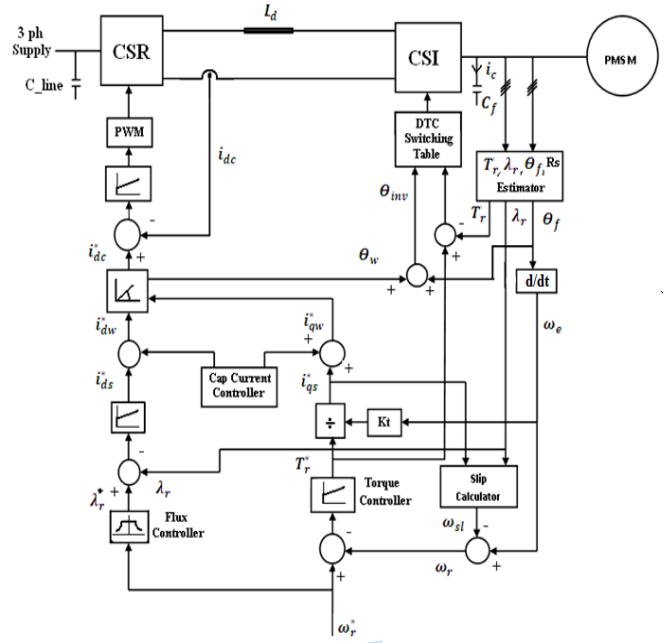


Figure 2. Functional block diagram of vector control CSI drive based for proposed configuration.

Speed Estimation

The motor speed estimated from the following

$$\omega_r = \omega_e - \omega_{sl} \quad (5)$$

Where

ω_e = Stator frequency in rad/sec

ω_{sl} = slip frequency in rad/sec

The motor parameters employed in the control system may deviate from the real ones.

CSI-fed motor drives have filter capacitors connected at the output of the inverter. This means that a portion of the inverter currents go through the capacitors. The influence of the filter capacitors on the system control is investigated in this section. The inverter reference currents can be expressed as follows [29]:

$$\begin{aligned} i_{dw}^* &= i_{cd} + i_{ds}^* \\ i_{qw}^* &= i_{cq} + i_{qs}^* \end{aligned} \quad (6)$$

where i_{cd} and i_{cq} are the estimated capacitor d , q -axis currents.

To reduce the sensitivity and noise caused by the derivative terms, the estimated capacitor currents are usually simplified as follows:

$$\begin{aligned} i_{cd} &= -\omega_e V_{qs} C_f \\ i_{cq} &= \omega_e V_{ds} C_f \end{aligned} \quad (7)$$

Where C_f , ω_e , v_{ds} , and v_{qs} are the inverter-side filter capacitance, motor electrical angular frequency, and stator d -axis and q -axis voltages, respectively.

DIRECT TORQUE CONTROLLER PRINCIPLE

The basic principle of DTC is to select stator current vectors according to the differences between the reference and actual torque and flux linkage. Stator flux and rotor flux are estimated from the Equation (8) (9), and (10) taking the integral of difference between the input voltage and the voltage drop across the stator resistance as,

$$\lambda_{ds} = \int (V_{ds} - \hat{R}_s i_{ds}) dt \tag{8}$$

$$\lambda_{qs} = \int (V_{qs} - \hat{R}_s i_{qs}) dt \tag{9}$$

$$\lambda_r = \int \frac{L_m}{L_r} [V_s - (\hat{R}_s + \sigma L_s p) i_s] \tag{10}$$

Where

- λ_{ds} - d-axis flux linkage.
- λ_{qs} - q-axis flux linkage.
- \hat{R}_s - estimated stator resistance.
- P - number of pole pairs

and then calculates the flux amplitude and find the sector of 60 degrees in α - β plane where flux vector resides, according to the partition shown in Figure 3.

In that case six intervals of 60 degrees can be defined in which the current and the voltage changes its values. In every interval the current from DC link flows through two inverter legs and two motor phase windings.

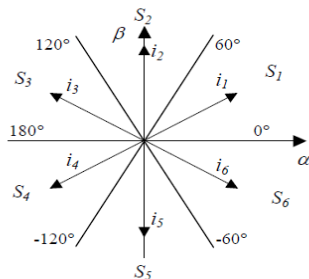


Figure 3. Sectors in $\alpha - \beta$ plane where rotor flux resides

From the stator output current and voltage, pure integrator in (1) and (2) yields flux vector. The trajectory of flux is exactly circular, it is important to note that the dynamics of stator flux estimation do not depend on the response of the offset estimator.

EFFECT OF STATOR RESISTANCE VARIATION

In DTC, the stator flux and rotor flux are estimated using the Equation (1) and (2) respectively. The variation of 'Rs' may influence the calculation of stator flux significantly and thereby the overall performance of the DTC system. At low speeds, the back EMF term is small, and the resistive drop 'Rs*Is' is comparable with the supply voltage magnitude 'Vs'. Therefore

any change in stator resistance gives wrong estimation of stator flux and consequently of the electric torque and the stator flux position. An error in stator flux position is more important as it can cause the controller to select a wrong switching state which can result in failure of the controller. At high speeds, the stator resistance drop 'Is*Rs' is small and can be neglected. If increase stator resistance the stator current, flux and torque are oscillated. So a mismatch between the set value and actual value can create instability. So the parameter mismatch between the controller and motor makes the drive system unstable. So the stator resistance compensation is essential to overcome instability in DTC controlled IM drive system.

Stator Resistance Compensation

An observer has been designed to estimate the change in the actual stator resistance during operation of the machine. The estimator observes if any change is detected, a corresponding change in the stator resistance is made. The available stator resistance on-line compensation schemes can be classified into a couple of distinct categories. The stator resistance on-line compensation method is by far the most frequently met and it includes all the estimators where an updated stator resistance value is obtained through an adaptive mechanism. Proportional integral (PI) or integral (I) controllers are used for this purpose. In MRAS based systems the rotor flux estimated from the reference model and adaptive model which is used to estimate the stator resistance. This paper analyses the stator resistance on-line compensation on PI control and MRAS control schemes, as discussed below.

PI Stator Resistance Estimator

The block diagram of PI stator resistance compensator is shown in Figure 4. The error in the stator flux is used as an input to the PI estimator. The technique is based on the principle that the change in stator resistance will cause a change in stator current and stator flux linkage λ_s . The error between the stator flux linkage λ_s and its reference λ_s^* is proportional to the stator resistance change. The equation for PI resistance estimator is given by

$$\Delta R_s = \left(K_p + K_I \frac{1}{s} \right) \Delta \lambda_s \tag{11}$$

Where, K_p and K_I are the proportional gain and integral gain of the PI estimator.

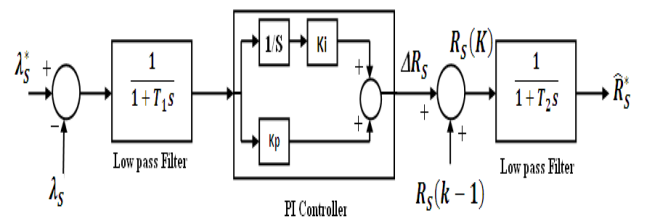


Figure 4. Block Diagram for PI Stator resistance compensation.

The error between the estimated stator flux λ_s and its reference λ_s^* is passed through a low pass filter with a very low cutoff frequency in order to attenuate high frequency component contained in the estimated stator flux. This filter time constant should be small compared to the stator resistance estimator time constant to overcome its effect on the stator resistance adaptation. Then the signal is passed through a PI estimator. The output of the PI estimator is the required change of resistance ΔR_s due to change in temperature or frequency. The change of stator resistance ΔR_s is continuously added to the previously estimated stator resistance $R_s(K-1)$. The final estimated stator resistance \hat{R}_s is again passed through a low pass filter to have a smooth variation of stator resistance value. This updated stator resistance can be used directly in the controller.

MRAS Based Control

The rotor speed and stator resistance estimation scheme is designed based on the concept of hyper stability [30] in order to make the system asymptotically stable. For the purpose of deriving an adaptation mechanism it is valid to initially treat rotor speed as a constant parameter, since it changes slowly compared to the change in rotor flux. The stator resistance of the motor varies with temperature, but variations are slow so that it can be treated as a constant parameter, too. The configuration of the proposed parallel rotor speed and stator resistance is shown in Fig. 5 and is discussed in detail next.

In this paper to analyze the speed estimator is originally proposed in [41] and illustrated in Figure 5, where the two left-hand side blocks perform integration of Equations (7) and (8). The reference (voltage) model and adjustable (current) models are derived by the stator voltage and currents. The estimator operates in the stationary reference frame (α) and it is described with the following equations [41]:

$$p\hat{\lambda}_{rV} = \frac{L_m}{L_r} [V_s - (\hat{R}_s + \sigma L_s p) \hat{i}_s] \quad (12)$$

$$p\hat{\lambda}_{rI} = \frac{L_m}{T_r} i_s \left(\frac{1}{T_r} - j\hat{\omega} \right) \hat{\lambda}_{rI} \quad (13)$$

$$\hat{\omega} = \left(K_{p\omega} + \frac{K_{I\omega}}{p} \right) e_\omega \quad (14)$$

$$e_\omega = \hat{\lambda}_{rI} \times \hat{\lambda}_{rV} = \hat{\lambda}_{\alpha I} \hat{\lambda}_{\beta rV} - \hat{\lambda}_{\beta rI} \hat{\lambda}_{\alpha V} \quad (15)$$

A symbol $\hat{}$ denotes in (12) - (15) estimated quantities, symbol ' p ' stands for d/dt , T_r is the rotor time constant and $\sigma = 1 - L_m^2 / L_s L_r$. All the parameters in the motor and the estimator are assumed to be of the same value, except for the stator resistance (hence a hat above the symbol in (12)). Underlined variables are space vectors, and sub-scripts V and I stand for the outputs of the voltage (reference) and current (adjustable) models, respectively. Voltage, current and flux are denoted with v , i and λ , respectively, and subscripts s and r stand for stator and rotor, respectively.

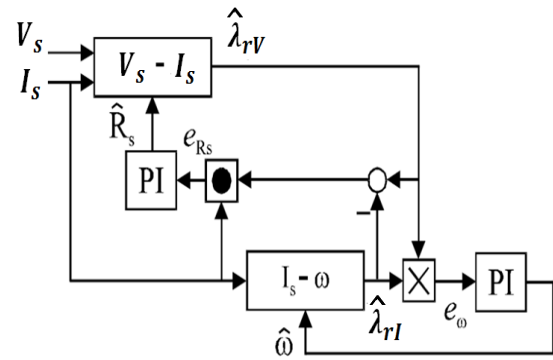


Figure 5. Structure of the MRAS system for parallel rotor speed and stator resistance estimation.

As is evident from (12)-(15) and Figure 5, the adaptive mechanism (PI controller) relies on an error quantity that represents the difference between the instantaneous positions of the two rotor flux estimates. The second degree of freedom, the difference in amplitudes of the two rotor flux estimates, is not utilized. The parallel rotor speed and stator resistance MRAS estimation scheme, which will be developed, will make use of this second degree of freedom to achieve simultaneous estimation of the two quantities. The role of the reference and the adjustable model will be interchanged for this purpose, since the rotor flux estimate of (13) is independent of stator resistance.

Let R_s and ω_r denote the true values of the stator resistance in the motor and rotor speed, respectively. These are in general different from the estimated values. Consequently, a mismatch between the estimated and true rotor flux space vectors appears as well. The error equations for the voltage and the current model outputs can then be written as;

$$p\underline{\varepsilon}_V = -\frac{L_r}{L_m} (R_s - \hat{R}_s) \hat{i}_s \quad (16)$$

$$\underline{\varepsilon}_V = \lambda_{rV} - \hat{\lambda}_{rV} = \varepsilon_{\alpha V} + j\varepsilon_{\beta V} \quad (17)$$

$$p\underline{\varepsilon}_I = \left(j\omega - \frac{1}{T_r} \right) \underline{\varepsilon}_I + j(\omega - \hat{\omega}) \hat{\lambda}_{rI} \quad (18)$$

$$\underline{\varepsilon}_I = \lambda_{rI} - \hat{\lambda}_{rI} = \varepsilon_{\alpha I} + j\varepsilon_{\beta I} \quad (19)$$

Symbols λ_{rV} , $\hat{\lambda}_{rV}$ in (17), λ_{rI} , $\hat{\lambda}_{rI}$ in (19) stand for true values of the two rotors flux space vectors which is obtained from reference model (V_s-I_s) and adaptive model ($\omega-I_s$) respectively. From equation (14) and (15) The adaptive mechanism for ω is obtained and for R_s estimation

$$\hat{R}_s = \left(K_{pRs} + \frac{K_{IRs}}{p} \right) e_{Rs} \quad (20)$$

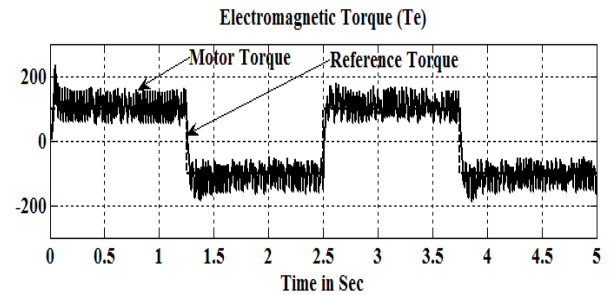
$$e_{Rs} = i_{\alpha s} (\psi_{\alpha rV} - \psi_{\alpha rI}) + i_{\beta s} (\psi_{\beta rV} - \psi_{\beta rI}) \quad (21)$$

are proposed by Popov's hyper stability theory.

RESULTS

Simulation Results

A sample of simulation results are presented here. Simulation results for a DTC system with resistance estimator were obtained using a 50-hp four-pole, induction machine. The machine parameters are shown in Appendix 1. The presented simulation results were made using MATLAB / Simulink software package. The sensor less DTC- CSI fed induction motor drive is operated with low speed with fast load changes is shown in Figure (6), is influence of inaccurate value of stator resistance. The estimation error is high and unstable in steady state and becomes higher at point of load changes. The simulation results of the presented control system with PI and MRAS estimated stator resistance tuning is shown in Figure (7) and (8) respectively. The actual and reference speed, torque, stator current and rotor flux are presented in Figure (7) and (8). The estimation error is very small and stable in steady state and becomes lower compared with stator resistance estimator is turned off at point of load changes



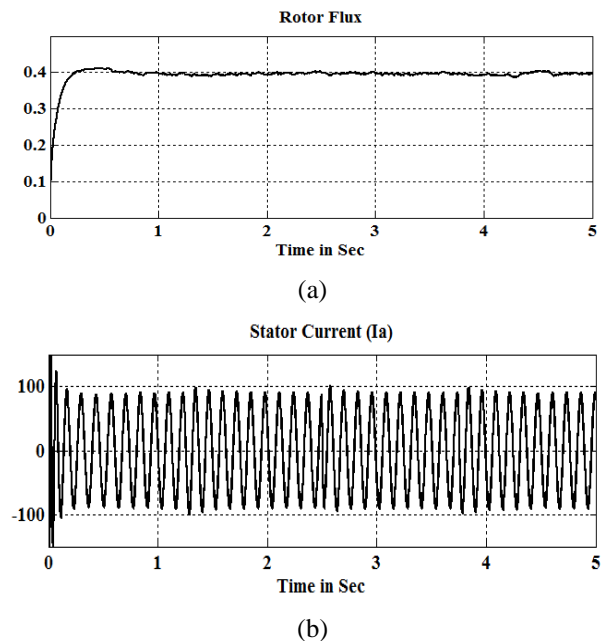
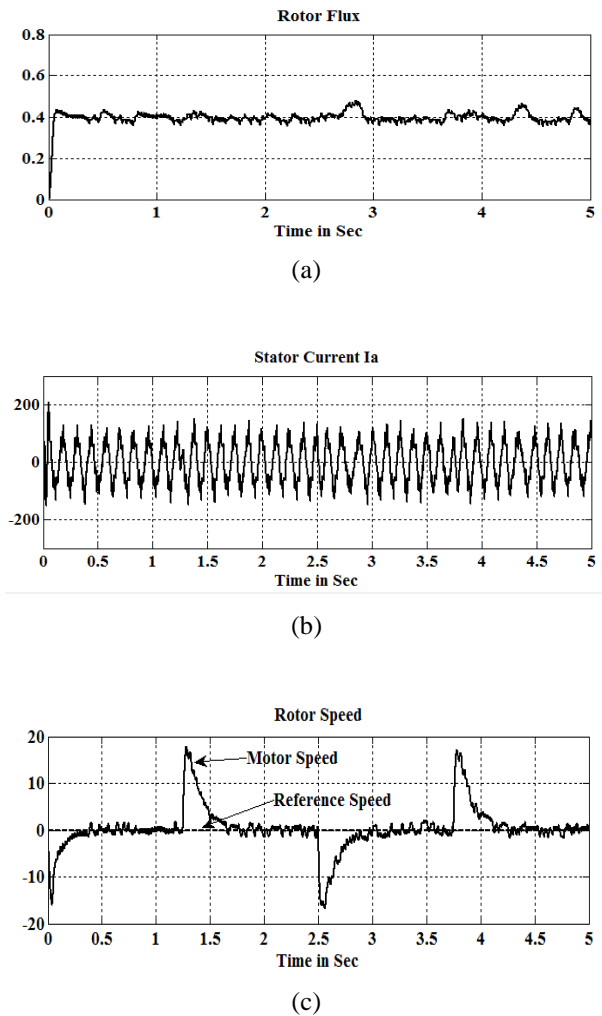
(d)

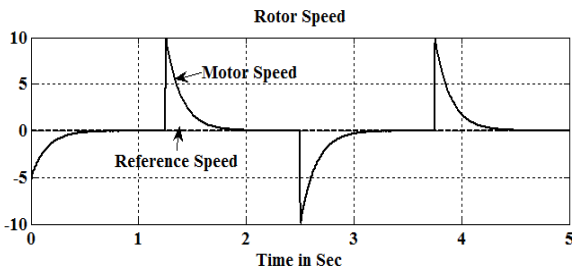
Figure 6. Without Rs Estimator (a) Rotor Flux (b) Stator Current (c) Rotor Speed (d) Torque

From the performance of the two estimators, it is obvious that the MRAS-based resistance estimator gives better tracking than the PI-based resistance estimator. Figure 9 shows the actual and estimated stator resistance of the machine with PI and MRAS estimator methods. In both methods, the estimated stator resistance follows very closely to the actual stator resistance of the machine. The MRAS estimator is able to estimate the resistance change better than the PI estimator.

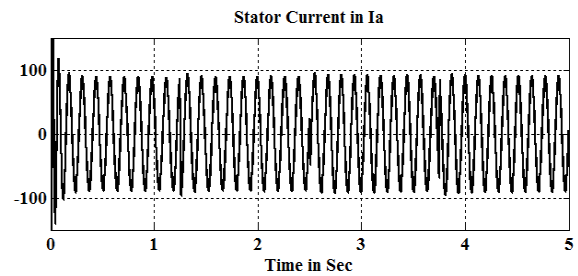
Experimental Results

Figure.10 shows a low-power prototype system is constructed for experimental verification with key parameters listed in Appendix 2. Although the rating of the laboratory prototype is lower than the practical high-power drive, their key parameters are similar. All measured and controller internal variables are accessible through the serial link to the PC.

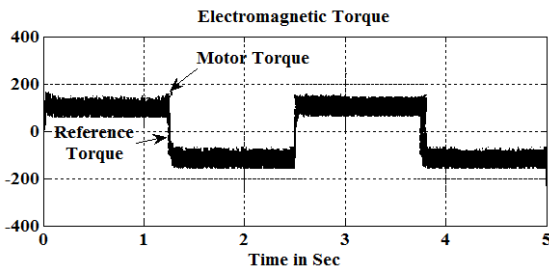




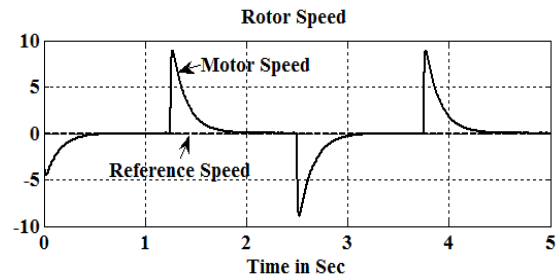
(c)



(b)



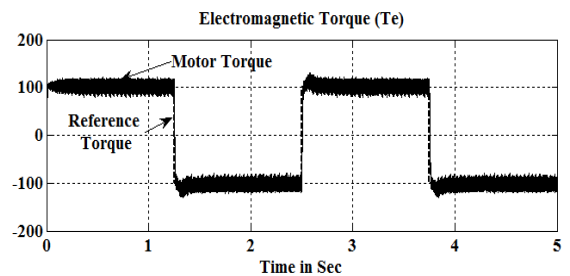
(d)



(c)

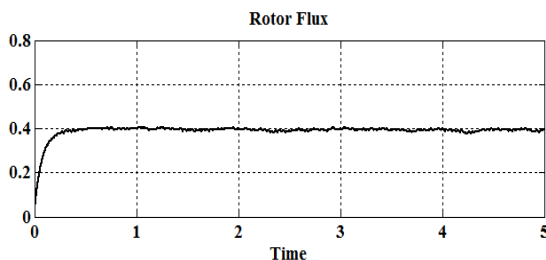
Figure 7. With PI Estimator (a) Rotor Flux (b) Stator Current (c) Rotor Speed (d) Torque

A dc motor is coupled to the shaft of the induction machine. It is supplied by a dc drive to generate the step load torque. The direct torque controller and resistance estimator were implemented with a single board computer that uses a 16-b TM320C14 digital signal processor (DSP). A 3-hp 420-V induction machine was used in the experiment. The stator resistance of the machine, calculated from tests on the machine, was found to be 0.435Ω . The machine currents and the dc bus voltage were interfaced into the controller through an analog-to-digital converter (A/D) built into the DSP board. The A/D and the multiplexer available were very slow. The command torque and command stator flux used are 11 Nm and 0.4 wb, respectively. The stator current vector at these values of command torque and command flux was found to be 10.4 A. The direct torque controller and the resistance estimator were programmed in assembly language. In actual operating conditions, the rate of change of temperature is very slow and so the stator resistance changes. Practically stator resistance changes in a nonlinear manner.



(d)

Figure 8. With MRAS Estimator (a) Rotor Flux (b) Stator Current (c) Rotor Speed (d) Torque



(a)

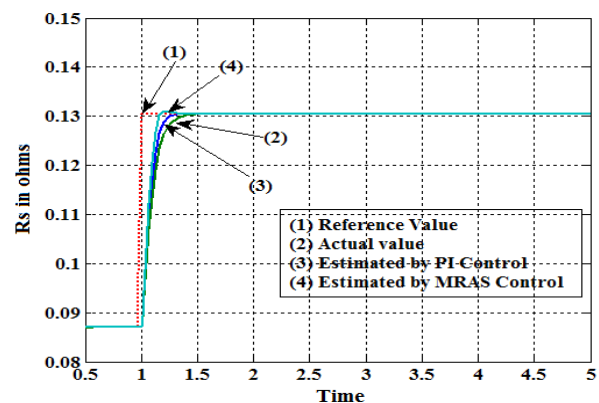


Figure 9. Rs Estimation

A linearly increasing resistance is simulated and Figure 13. Figure 11 and 12 shows that the stator current, Speed and Torque response of CSI fed Induction motor drive with a stator resistance compensated by PI and MRAS respectively.

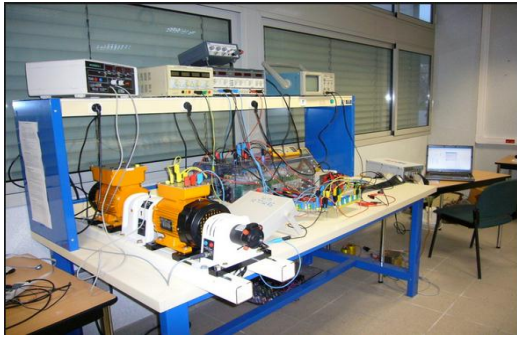
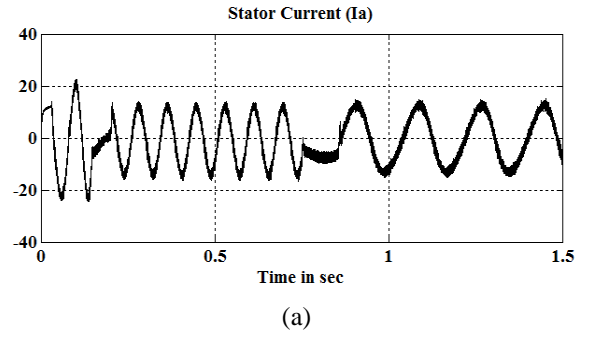
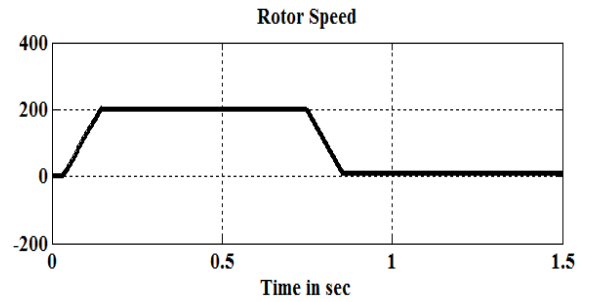


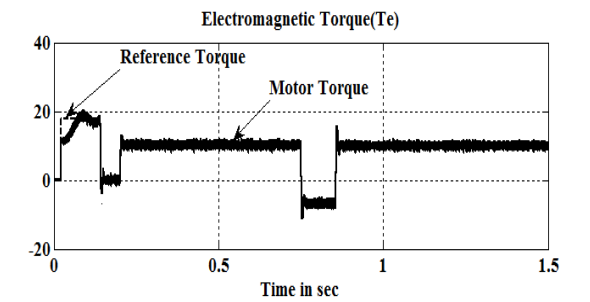
Figure 10. Experimental setup



(a)

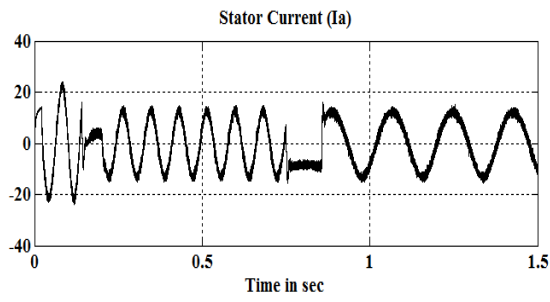


(b)

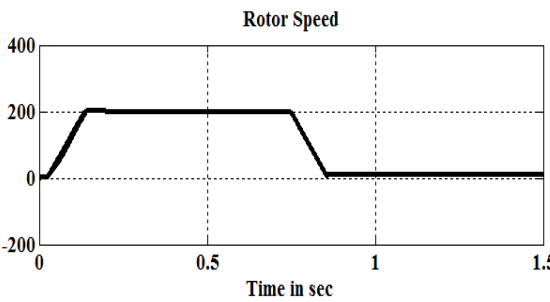


(c)

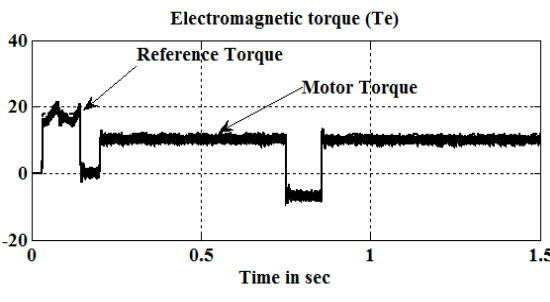
Figure 12. Experimental results with MRAS Estimator (a) Stator Current (b) Rotor Speed (200rpm-10rpm) (c) Torque



(a)



(b)



(c)

Figure 11. Experimental results with PI Estimator (a) Stator Current (b) Rotor Speed (200rpm-10rpm) (c) Torque

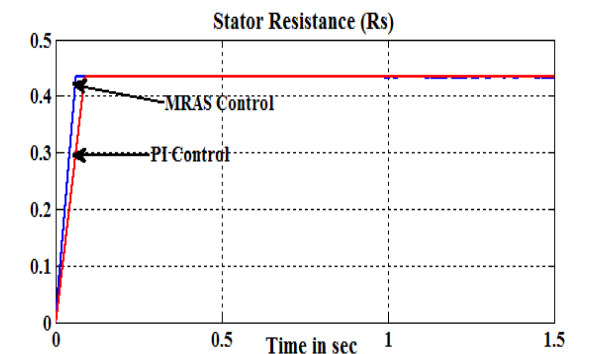


Figure 13. R_s estimation with PI and MRAS Control when increases linearly.

CONCLUSION

The stator resistance has been estimated by using PI controller and MRAS controller and performance of controller analyzed during low speed operations of CSI fed drives. The simulation and experimental results shows that both estimators are able to compensate for the changes in stator resistance. The MRAS resistance estimator showed a better performance than the PI estimator. Also, robustness and ability to operate the controller with MRAS resistance estimator at very low speeds has also been shown experimentally.

APPENDIX 1 INDUCTION MOTOR PARAMETERS

Rated Power	:50 hp
Rated Voltage	: 460 V
Stator Resistance	: 0.087 Ω
Stator Inductance	: 35.5 mH
Rotor Resistance	: 0.228 Ω
Rotor Inductance	: 35.5 mH
Mutual Inductance	: 34.7 mH
Moment of inertia	: 1.662 kg.m ²
Friction co efficient	: 0.1 N.m.s/rad
Number of poles	: 4

APPENDIX 2 KEY PARAMETERS OF THE EXPERIMENT SETUP

Rated Power	:3 hp
Rated Voltage	:208 V
Stator Resistance	:0.435 Ω
Rotor Resistance	:0.816 Ω
Stator Inductance	:71.31 mH
Rotor Inductance	:71.31 mH
Mutual Inductance	:69.31 mH
Moment of inertia	:0.089 kg.m ²
Friction co efficient	:0.005 .m.s/rad
Number of poles	:4

REFERENCES

- [1] Joshi, R.R., Gupta, R.A & Wadhvani A.K.,2007, "Experimental Investigation on Ride through Capability of Closed Loop Controlled Matrix Converter Fed Cage Drive," IETE Technical Review Volume 24, Issue 2.
- [2] Beig, R and Ranganathan, V T., 2002 "A novel CSI-fed induction motor drive," *IEEE Trans. Power Electron.*, vol. 21, no. 4, pp. 1073–1082,
- [3] Ojo.,O and Vanaparthi, S,2004., "Carrier-based discontinuous PWM modulation for current source converters," in *Conf. Rec. IEEE IAS Annu. Meet. 2004*, Oct. 3–7, vol. 4, pp. 2224–2231.
- [4] Halkosaari, T and Tuusa, H., 2002 "Optimal vectormodulation of a PWM current source converter according to minimal switching losses," in *Proc. IEEE PESC*, pp. 127–132.
- [5] Wiechmann, E. P., Burgos, R. P., and Holtz J.,2003., "Active front-end converter for medium-voltage current source drives using sequential-sampling synchronous space-vector modulation," *IEEE Trans. Ind. Electron.*, vol. 50, no. 6, pp. 1275–1289, Dec. 2003.
- [6] Holtz J and Oikonomou N.,2007., "Synchronous optimal pulse width modulation and stator flux trajectory control for medium-voltage drives,"*IEEETrans.Ind.Appl.*,vol.43,no.2,pp.600–608,Mar./Apr.2007.
- [7] Li, Y. W., Wu, B., Xu D., and Zargari N.,2008 "Space vector sequence investigation and synchronization methods for active front-end rectifiers in high-power current-source drives," *IEEE Trans. Ind. Electron.*, vol. 55, no. 3, pp. 1022–1034,
- [8] Rodríguez, J., Morán, L., Pontt, J., Osorio, R., and Kouro, S.,2003, "Modeling and analysis of common-mode voltages generated in medium voltage PWM CSI drives,"*IEEETrans. PowerElectron.*, vol.18,no.3,pp.873–79.
- [9] Nikolic and Jefienic B.,2004, "Speed sensorless direct torque control implementation in a current source inverter fed induction motor drive," in *Proc. IEEE—PESC*, vol. 4, pp. 2843–2848.
- [10] Rees, S. and Ammann U.,2004., "New stator voltage controller for high speed induction machines fed by current-source inverters," in *Proc. IEEE PESC*, Jun. 20–25, vol. 1, pp. 541–547.
- [11] Pankaj Swarnkar, Shailendra Kumar Jain and Nema, R.K.,2014 " Adaptive Control Schemes for Improving the Control System Dynamics: A Review", IETE Technical Review, Volume 31, Issue 1, pp 17-33.
- [12] Suh Y., Steinke J., and P. Steimer, 2006, "A study on efficiency of voltage source and current source converter systems for large motor drives," in *Proc. 37th IEEE Power Electron. Spec. Conf.*, pp. 1–7.
- [13] Wiechmann E. P., Aquevenque P., Burgos R., and Rodriguez J.,2008, "On the efficiency of voltage source and current source inverters for high-powerdrives,"*IEEETrans.Ind.Electron.*,vol.55,no.4,pp .1771–1782.
- [14] Habetler, T. and Divan, D.,1991, "Control strategies for direct torque control of induction machines using discrete pulse modulation," *IEEE Trans. Ind. Applicat.*, pp. 893–901.
- [15] Rajashekara K., Kawamura A., and Matsuse K.,1996 (editors), *Sensorless control of AC motor drives*, IEEE Press.
- [16] Panneer Selvam N., and Rajasekaran V, 2014 "High Performance operations of DTC-CSI fed IM Drives at low speed with On Line Stator resistance

- Compensation,” in *International journal of Applied Engineering Research*, Vol 9, pp 19211-19230.
- [17] Ha, I. J., and Lee, S. H., 2000 “An online identification method for both stator and rotor resistance of induction motors without rotational transducers,” *IEEE Trans. on Industrial Electronics*, vol. 47, no. 4, pp. 842-853.
- [18] Tsuji, M., Chen, S., Izumi, K., and Yamada E., 2001, “A sensorless vector control system for induction motors using q-axis flux with stator resistance identification,” *IEEE Trans. on Industrial Electronics*, vol. 48, no. 1, pp. 185-194.
- [19] Akatsu K., and Kawamura A., 2000, “Sensorless very low-speed and zero-speed estimations with online rotor resistance estimation of induction motor without signal injection,” *IEEE Trans. on Industry Applications*, vol. 36, no. 3, pp. 764-771, 2000.
- [20] Marino, R., Peresada, S., and Tomei, P., 2000, “On-line stator and rotor resistance estimation for induction motors,” *IEEE Trans. on Control Systems Technology*, vol. 8, no. 3, pp. 570-579.
- [21] Guidi, G., and Umida H., 2000, “A novel stator resistance estimation method for speed-sensorless induction motor drives,” *IEEE Trans. on Industry Applications*, vol. 36, no. 6, pp. 1619-1627.
- [22] Shinohara, K., Nagano, T., Arima H., and Mustafa, W.Z.W., 2001, “Online tuning method of stator and rotor resistances in both motoring and regenerating operations for vector controlled induction machines,” *Electrical Engineering in Japan*, vol. 135, no. 1, pp. 56-64.
- [23] Mitronikas, E. D., Safacas, A. N., and Tatakis E. C., 2001, “A new stator resistance tuning method for stator-flux-oriented vector-controlled induction motor drive,” *IEEE Trans. on Industrial Electronics*, vol. 48, no. 6, pp. 1148-1157.
- [24] Jarray, K., Boussak, M., and Tholomier M., 2000, “Stator resistance tuning in sensorless stator-flux field-oriented induction motor drive,” in *Proc. Int. Conf. on Electrical Machines ICEM*, pp. 543-547.
- [25] Raison, B., Arza, J., Rostaing, G., and Rognon J. P., 2000, “Comparison of two extended observers for the resistance estimation of an induction machine,” in *Proc. IEEE Ind. Appl. Soc. Annual Meeting IAS*, Paper no. 32_06.
- [26] Hamajima, T., Hasegawa, M., Doki, S., and Okuma, S., 2002, “Sensorless vector control of induction motor with stator resistance identification based on augmented error,” in *Proc. Power Conversion Conf.*, pp. 504-509.
- [27] Campbell, J., and Sumner, M., 2002, “Practical sensorless induction motor drive employing an artificial neural network for online parameter adaptation,” *IEE Proc. – Electr. Power Appl.*, vol. 149, no. 4, pp. 255-260.
- [28] Halkosaari, T., and Tuusa, H., 1999, “Reduction of conducted emissions and motor bearing currents in current source PWM inverter drives,” in *Proc. 30th Annu. IEEE Power Electronics Specialists Conf.*, vol. 2, pp. 959-964 .
- [29] B. Wu, 2006,. “*High-Power Converters and AC Drives*”. Hoboken, NJ: Wiley,
- [30] Schauder C., 1992, “Adaptive speed identification for vector control of induction motors without rotational transducers,” *IEEE Trans. On Industry Applications*, vol. 28, no. 5, pp. 1054-1061.